Electroforming of oxide-nanoparticle-reinforced copper-matrix composite

Satoshi Semboshi[a)]
Kansai Center, Institute for Materials Research, Tohoku University, Sakai, Osaka 599-8531, Japan; and Department of Materials Science, Osaka Prefecture University, Sakai, Osaka 599-8531, Japan

Yasuhiro Sakamoto
Research Organization for the 21st Century, Osaka Prefecture University, Sakai, Osaka 599-8531, Japan

Hiroyuki Inoue and Akihiro Iwase
Department of Materials Science, Osaka Prefecture University, Sakai, Osaka 599-8531, Japan

Naoya Masahashi
Kansai Center, Institute for Materials Research, Tohoku University, Sakai, Osaka 599-8531, Japan

(Received 9 June 2014; accepted 12 November 2014)

A method based on the electroforming technique has been proposed for the fabrication of nanoparticle-reinforced copper-matrix composites using an electrolyte of copper sulfate–sulfuric acid solution containing 1 cm^3/L of the nanoparticles without surfactants. Of the tested nanoparticles such as Al_2O_3, SiO_2, TiO_2, ZrO_2, and CeO_2, whose sizes ranged from 10 to 30 nm, only TiO_2 nanoparticles were successfully embedded in the copper matrix during electroforming, owing to their positive charge in the electrolyte solution. It should be noted that there was very little contamination in the copper matrix, because surfactants were absent during electroforming. Therefore, the electrical conductivity of the specimen that was electroformed in the electrolytes with TiO_2 nanoparticles was not significantly different from that of pure copper. Nevertheless, the hardness, yield, and ultimate tensile strength were significantly improved by a small amount (0.3 mass%) of TiO_2 nanoparticles primarily because of strengthening by Orowan mechanics. The electroforming process is thus a promising means to prepare copper-matrix composites with an excellent balance of electrical conductivity and mechanical strengths.

I. INTRODUCTION

The use of copper in power-supply interconnections such as electric cables and connectors requires not only excellent electrical conductivity but also good mechanical properties. The mechanical properties of soft copper are typically improved through alloying with metallic elements and thermomechanical processing, as this leads to solid-solution and age-precipitation strengthening. However, even just a small amount of solid-solution metal alloying significantly increases the electrical resistivity of copper.[1–3] There is, therefore, a need for new techniques and processes to improve the mechanical properties of copper without degrading its electrical conductivity.

An attractive solution to this problem lies in pure copper-based composites that are strengthened by a fine dispersion of hard and inert particles. Since the copper matrix retains essentially the same electrical conductivity as that of the pure metal, the decrease in conductivity of the composite is limited to just a few percent by virtue of the small volume fraction of added particles. Moreover, the mechanical properties are enhanced by the hard nanoparticles, ideally measuring several tens of nanometers in diameter, through an Orowan mechanism[4,5] that is similar to conventional age-precipitation strengthening.

Various processes have been proposed for fabricating bulk-copper-matrix composites, including melting and casting-based processes,[6–9] internal oxidation methods,[6,10,11] powder metallurgical techniques,[6,12–14] and electroforming-based procedures.[6,15–18] The latter have evolved from the principles of electroplating and electrodeposition, and they provide the ability to embed inert particles suspended in an electrolyte solution in a metal matrix during electrolysis. Composite electroforming offers two advantages. First, a high-purity metal matrix can be easily prepared, particularly in the case of copper, and it helps preserve the electrical conductivity. Second, the electroformed composites have the potential to host a uniform dispersion of inert particles, which is an important feature as it can help attain sufficient mechanical strengthening.

There have been a number of previous reports pertaining to the dispersion of microscale and submicroscale inert particles, including SiC,[19] Al_2O_3,[20,21] TiO_2,[22] CeO_2,[23] and so on,[24,25] into a metal matrix such as copper or nickel

Contributing Editor: Jürgen Eckert
[a)]Address all correspondence to this author.
e-mail: semboshi@imr.tohoku.ac.jp
DOI: 10.1557/jmr.2014.401

 © Materials Research Society 2015

https://doi.org/10.1557/jmr.2014.401 Published online by Cambridge University Press

by electroforming. More recently, the size of these inert particles has been reduced from several micrometers to tens of nanometers in a bid to further improve the mechanical and physical performance of the resulting composite. From a practical perspective, however, it is difficult to obtain a uniform dispersion of fine particles (<100 nm) in the matrix using electroforming. This is often attributed to the effects of particle aggregation and the surface potential of nanoparticles in the electrolyte solution, although inert particles have been successfully kept in suspensions during electroplating and electroforming through either mechanical stirring or using appropriate organic surfactants, such as fluorocarbon or gelatin.[17,18,20–25] With the use of surfactants, however, a large amount of impurities in the form of carbon and oxygen are present in the final composites, resulting in serious embrittlement of the materials.[6,18,26] Thus, although the use of organic surfactants in suspensions may be useful in the case of electroplated surface coatings for wear resistance, their use should be avoided when fabricating bulk composites where high toughness and high electrical conductivity are required.

In this study, we aimed to fabricate bulk copper-matrix composites reinforced with oxide nanoparticles by using an electrolyte without surfactants to avoid contamination. To this end, a range of nanoparticles were tested (Al_2O_3, SiO_2, TiO_2, ZrO_2, and CeO_2) to find the one most suitable for this procedure. The mechanical properties and electrical conductivity of the resulting composites were examined; based on the results, the critical factor that governs the electroforming of copper-matrix composites with nanoparticles is discussed here.

II. EXPERIMENTAL

The electrolyte used in this study was a copper sulfate–sulfuric acid solution, which consisted of pure water (1000 mL), copper sulfate (140 g), and sulfuric acid (70 mL). The pH value of the electrolyte was approximately 0.4. Nanoparticles of Al_2O_3, SiO_2, TiO_2, ZrO_2, or CeO_2 were added to the electrolyte at a concentration of 1 cm^3/L (i.e., the volume density of the oxide). The mean size of these nanoparticles ranged from 10 to 30 nm, and a representative micrograph of TiO_2 nanoparticles is shown in Fig. 1. The resulting electrolyte mixtures were agitated by magnetic stirring at a speed of 250 revolutions per minute (rpm) to suppress settling of the nanoparticles; they were stabilized for approximately 3 h prior to electroforming. The cathode plate ($80 \times 40 \times 0.5$ mm^3; type 304 stainless steel) for electroforming was thoroughly washed using ethanol, and then rinsed with distilled water. Insulating tape was then used to tightly cover all but a 40×30 mm^2 electroforming area of the cathode plate. The anode plate ($80 \times 40 \times 1.5$ mm^3 phosphor copper) was submerged in dilute nitric acid for a few minutes to remove the surface contamination, and then rinsed with distilled water. It should be noted that in a preliminary experiment, we confirmed that the components used in electroforming, such as the nanoparticles, stainless steel, and insulating tape, were resistant to decay in the acid electrolyte over test periods of at least three days. This means that no reaction should occur in the system without applying an electrical charging. Electroforming was performed over 24 h using an applied current density of 0.5 mA/mm^2 (i.e., an applied current of 0.6 A was applied to the 40×30 mm^2 electroforming area); agitation was realized by magnetic stirring at a speed of 250 rpm. The electrolyte temperature was maintained at 298 K.

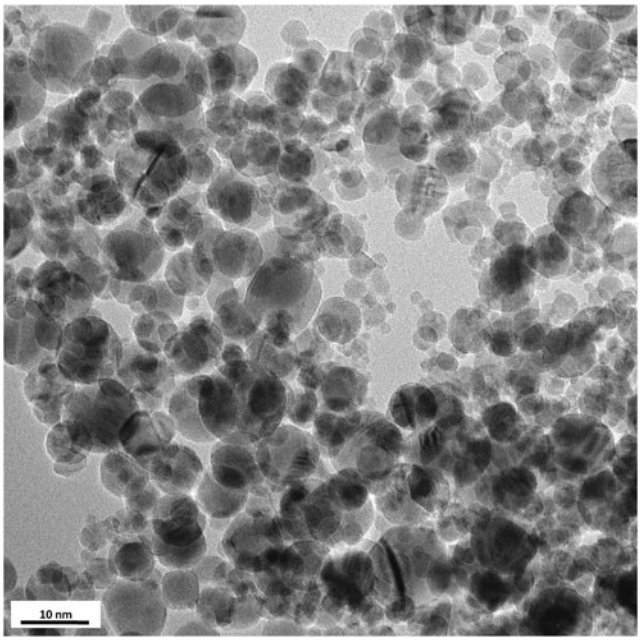


FIG. 1. TEM image of a typical TiO_2 nanoparticle used in this study.

The composition of metallic elements, sulfur, and phosphor in the electroformed specimens was determined through inductively coupled plasma-optical emission spectrometry (IRIS Advantage DUO, Thermo Fisher Scientific, Waltham, MA). The oxygen content was obtained through helium-carrier fusion thermal-conductivity measurements (TC-436, LECO, St. Joseph, MI). The microstructures of the electroformed specimens were observed using a transmission electron microscope (TEM; JEM3010, JEOL, Tokyo, Japan) operated at 300 kV. Samples for TEM observations were prepared from thin foils ground to less than 50 μm in thickness. The ground samples were then subjected to low-angle ion milling (GATAN, PIPS Model 691, Tokyo, Japan) using an argon ion beam accelerated by voltages below 3 kV. High-purity (99.9999 mass% pure) argon gas was used as the ion-beam source.

To examine the electrical charge of the oxide nanoparticle surface in the electrolyte, measurements of

https://doi.org/10.1557/jmr.2014.401 Published online by Cambridge University Press

surface potential, i.e., zeta potential, were carried out at 298 K using a zeta potential analyzer (ELSZ-1000ZS, Otsuka Electronics Co. Ltd., Osaka, Japan). It should be noted that before the measurement, the electrolytes were passed once through a filter with a pore diameter of 30 μm to remove the aggregated powder. The values of zeta potential were obtained by averaging the results of five measurements; the maximum and minimum values were excluded. The Vickers hardness of the electroformed specimens was measured by applying a load of 4.9 N and holding it for 10 s. All hardness values obtained were based on an average of values from 12 indentations; the maximum and minimum values were excluded from this calculation. Tensile tests were performed at 298 K using a universal tensile testing machine (TENSIRON UTA-10 KN, A&D Co. Ltd., Tokyo, Japan) and a strain rate of 1.67×10^{-4} s^{-1}. Tensile-test specimens measuring 10 mm in length, 1.7 mm in width, and 0.7–1.0 mm in thickness (obtained with a gauge) were cut from the electroformed specimens using electrical-discharge machining (EDM), and their surfaces were mechanically polished using diamond slurry. Three tensile tests were performed for each specimen. The electrical resistivity was measured at 298 K using a constant-DC-current four-terminal technique (current: 100 mA). For these measurements, the electroformed specimens were first cold-rolled and then cut by EDM to a size of $80 \times 2 \times 0.2$ mm^3.

III. RESULTS AND DISCUSSION

A. Nanoparticle selection for fabrication of copper-matrix composite

During electroforming at a current density of 0.5 mA/mm^2, it appeared that the copper film was deposited and grown on the type 304 stainless steel cathode without H_2 bubbling. After electroforming for 24 h, bulk copper specimens with a thickness of approximately 1.5 mm were formed on the cathode, regardless of whether the electrolyte contained oxide nanoparticles. After electroforming, the copper specimens were easily separated from the cathode, which was not corroded after electroforming. The current efficiency to electroform the copper-matrix composites was calculated from its weight to be almost 100%. As reported previously,[21,27] all of the electroformed specimens had some nodular units and rough surfaces. Hereafter, the copper specimen electroformed in the electrolyte without oxide nanoparticles is referred to as EF-Cu, and the specimens electroformed in the electrolytes with Al_2O_3, SiO_2, TiO_2, ZrO_2, and CeO_2 particles are referred to as EF-Cu/Al_2O_3, EF-Cu/SiO_2, EF-Cu/TiO_2, EF-Cu/ZrO_2, and EF-Cu/CeO_2, respectively.

Table I lists the concentration of oxygen, sulfur, phosphor, and metallic element in the oxide nanoparticles presented in the electroformed specimens. This indicates that the Cu content of the EF-Cu specimen was greater than 99.98 mass%, with the sulfur and phosphor content below the detectable limit. The oxygen content was measured as 170 ppm, which is similar to the value for commercial tough-pitch copper. In the EF-Cu/SiO_2, EF-Cu/ZrO_2, and EF-Cu/CeO_2 specimens, the concentrations of oxygen, sulfur, and phosphor were all similar to those of the EF-Cu specimen; however, the concentrations of the metallic elements in the oxide (i.e., Si, Zr, and Ce) were below the detection limit of 0.005 mass%. This suggests that these particular electroformed specimens did not contain any significant distribution of oxide nanoparticles. In the EF-Cu/Al_2O_3 and EF-Cu/TiO_2 specimens, the concentrations of Al and Ti in the oxides were found to be 0.020 and 0.176 mass%, respectively. If we assume that all of the metallic elements were contained within oxide nanoparticles dispersed in the EF-Cu/Al_2O_3 and EF-Cu/TiO_2 specimens, the amount of oxide nanoparticles in each specimen can be estimated as 0.038 and 0.294 mass%, respectively. Note that the concentrations of oxygen in the matrices of the EF-Cu/Al_2O_3 and EF-Cu/TiO_2 specimens were also estimated, as shown in Table I; these values are not considerably different from those of the other electroformed specimens.

Figures 2(a)–2(f) show typical bright-field TEM images of the electroformed specimens. The TEM image of the EF-Cu specimen in Fig. 2(a) shows fine grains of copper, and their mean size of several hundred nanometers was much smaller than those in conventionally annealed pure copper (several tens to hundreds of micrometers). This is in agreement with previous reports[28,29]; the other electroformed specimens exhibited similar fine grain size [Figs. 2(b)–2(f)]. TEM observation failed to identify any nanoparticles in the EF-Cu/SiO_2, EF-Cu/ZrO_2, and EF-Cu/CeO_2 specimens, as shown in Figs. 2(c), 2(e), and 2(f), respectively. On the other hand, nanoparticles measuring a few tens of nanometers in diameter were found to be dispersed in the copper matrix in the EF-Cu/Al_2O_3 and EF-Cu/TiO_2 specimens, as shown in Figs. 2(b) and 2(d). Interestingly, the quantity of nanoparticles in the EF-Cu/TiO_2 specimen was greater than that in the EF-Cu/Al_2O_3 specimen, although their distribution was less uniform. These observations are consistent with the results of the chemical analysis listed in Table I. It is therefore concluded that it is possible to efficiently fabricate copper-matrix composites with dispersed oxide nanoparticles through electroforming when TiO_2 nanoparticles are used in the electrolyte. Conversely, copper-matrix composites containing SiO_2, ZrO_2, or CeO_2 nanoparticles are not readily achieved by electroforming when a surfactant-free electrolyte is used.

Among possible mechanisms proposed for the electroforming of copper with inert particles, a few have

https://doi.org/10.1557/jmr.2014.401 Published online by Cambridge University Press

TABLE I. Chemically analyzed concentration of metallic elements, oxygen, sulfur, and phosphorus in the electroformed specimens; the estimated concentration of oxide nanoparticles and oxygen in the electroformed specimens.

	Chemically analyzed concentration				Estimated concentration	
Specimen	Metallic element (mass%)	O (mass%)	S (ppm)	P (ppm)	Oxide particle (mass%)	Oxygen in matrix (mass%)
EF-Cu	...	0.017 ± 0.004	<5	<100	...	0.017
EF-Cu/Al_2O_3	0.020 ± 0.002	0.026 ± 0.003	9 ± 1	<100	0.038	0.008
EF-Cu/SiO_2	<0.005	0.010 ± 0.001	6 ± 1	<100	<0.010	0.004
EF-Cu/TiO_2	0.176 ± 0.001	0.127 ± 0.012	31 ± 2	<100	0.294	0.009
EF-Cu/ZrO_2	<0.005	0.015 ± 0.001	<5	<100	<0.003	0.004
EF-Cu/CeO_2	<0.005	0.017 ± 0.001	6 ± 1	<100	<0.006	0.007

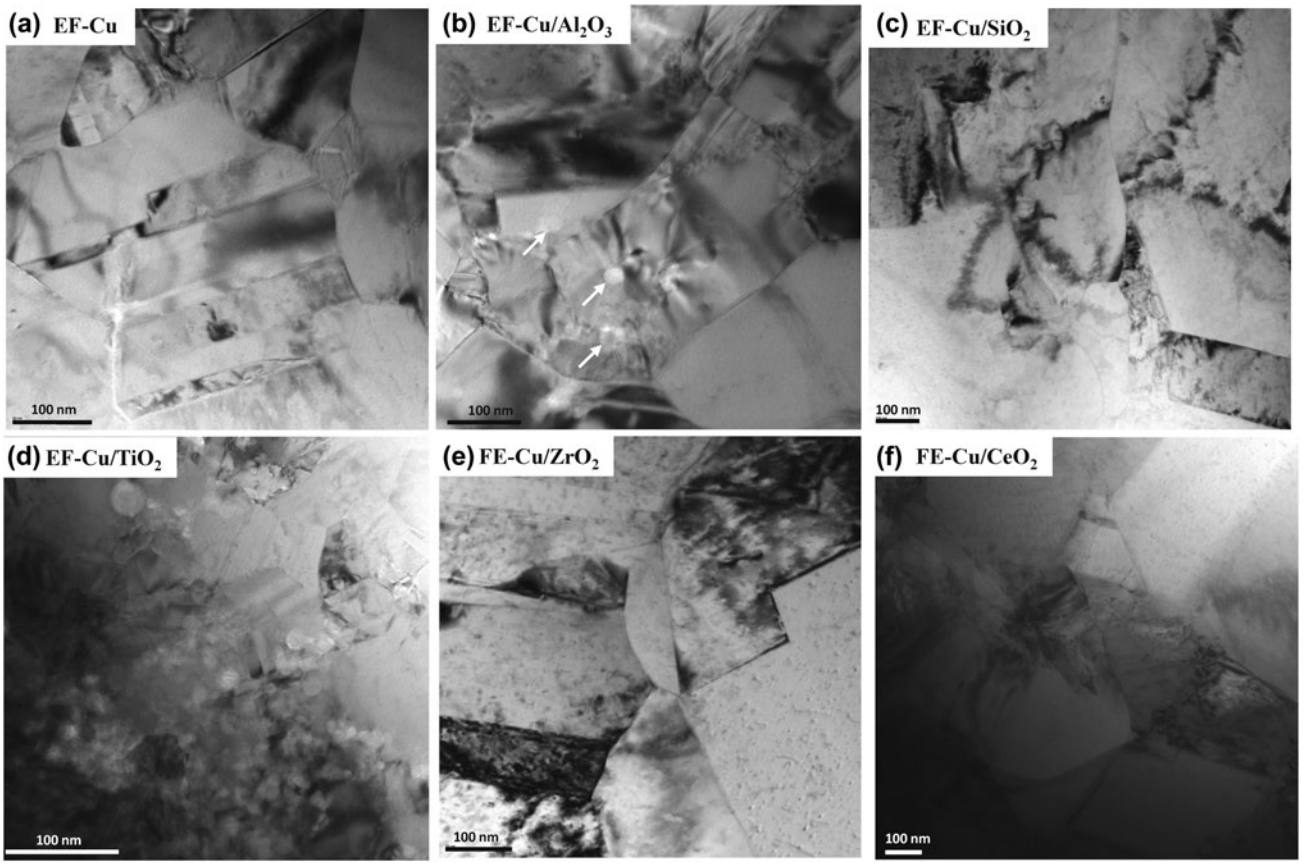


FIG. 2. TEM images of (a) EF-Cu, (b) EF-Cu/Al_2O_3, (c) EF-Cu/SiO_2, (d) EF-Cu/TiO_2, (e) EF-Cu/ZrO_2, and (f) EF-Cu/CeO_2 composites.

generally been accepted.[16] In the first scenario, particles migrate to the cathode via an electrophoretic action and are therefore embedded in the copper during electroforming. Alternatively, particles may be brought to the cathode by agitation and become mechanically entrapped in the copper. In the present study, the fact that the electrolyte solution was stirred at a constant rate (250 rpm) should pose little difference in mechanical agitation of various electroforming specimens. Consequently, the electrophoretic action of nanoparticles in the electrolyte solution is considered to be the more critical factor.

To further explore the contribution of this electrophoretic action to the fabrication of copper-matrix composites by electroforming, we examined the zeta potential of nanoparticles in the electrolyte solution. The values obtained are listed in Table II, which also includes previously reported zeta potentials for TiO_2 and ZrO_2 (Ref. 30–32) in a solution with a similar pH value for comparison. The values show a significant variation in the measured zeta potential values, which is probably attributable to particle aggregation in the electrolyte. However, it can be qualitatively stated that the SiO_2, ZrO_2, and CeO_2 nanoparticles exhibited negative values in zeta potential for the electrolyte solution, whereas the TiO_2 nanoparticles had a positive value. In the case of the Al_2O_3 nanoparticles, the

https://doi.org/10.1557/jmr.2014.401 Published online by Cambridge University Press

TABLE II. Zeta potential of nanoparticles in the copper sulfate–sulfuric acid solution.

Particles	Measured zeta potential (mV)	Reported zeta potential (mV)
Alumina, Al_2O_3	−6 ± 22	...
Silica, SiO_2	−46 ± 23	...
Titania, TiO_2	25 ± 14	>20 (Ref. 30), 30–40 (Ref. 31)
Zirconia, ZrO_2	−59 ± 30	−10 to −5 (Ref. 32)
Ceria, CeO_2	−30 ± 16	...

polarization of the surface potential is believed to have been near neutral. These zeta potential data therefore closely reflect the codeposition by electroforming, i.e., only nanoparticles with a positive charge in the electrolyte followed the copper ions in the migration to the cathode during electroforming. Therefore, when selecting nanoparticles for dispersion in a copper-matrix composite, a positive surface potential in the electrolyte solution should be considered as one of the most critical factors.

It should be noted that the magnitude of the zeta potential of nanoparticles in the electrolyte solution is a significant measure of the solution stability. Lower values toward zero, regardless of whether they are positive or negative, indicate an unstable solution with a tendency to flocculate because of the small electrostatic repulsive force among the nanoparticles. All the zeta potentials measured in this study showed relatively low magnitudes (see Table II), which means that it was difficult for the nanoparticles to disperse homogeneously in the solution without agitation. Therefore, it is important to understand how an electrolyte solution can be agitated during electroforming; this topic will be discussed in a future paper.

B. Electrical and mechanical properties

The electrical conductivity and Vickers hardness of the electroformed specimens are shown in Fig. 3. Here, the conductivity is expressed in terms of "% IACS", which is defined as the percentage of an International Annealed Copper Standard at 298 K, $5.8 \times 10^7\ \Omega^{-1}\ m^{-1}$. The conductivity of the EF-Cu specimen, 96 ± 5% IACS, is close to that of pure copper (100% IACS); the conductivities of the other electroformed specimens were at a slightly lower level, but within the margin of experimental accuracy. These high values can be attributed to the low concentration of contaminants such as oxygen, sulfur, and phosphor in the copper matrix of the electroformed specimens, as demonstrated in Table I. Figure 3(a) indicates that the TiO_2 nanoparticles contained in the EF-Cu/TiO_2 specimen had little overall effect on the electrical conductivity of the composite, despite the electrical conductivity of TiO_2 (10^{-8}–$10^{-10}\ \Omega^{-1}\ m^{-1}$) being much

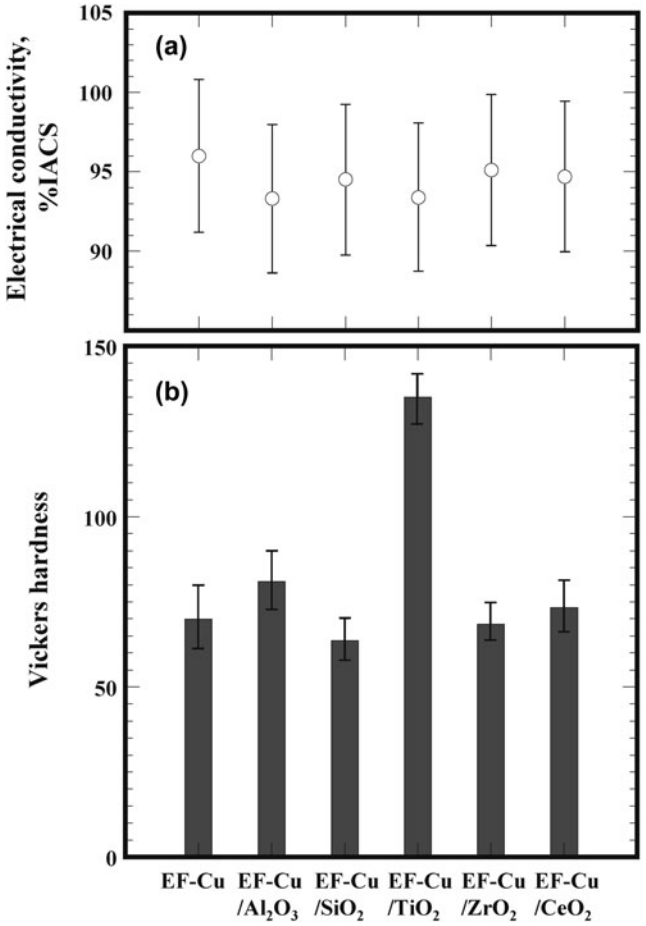


FIG. 3. (a) Electrical conductivity and (b) Vickers hardness of the electroformed composites.

lower than that of pure copper, $5.8 \times 10^7\ \Omega^{-1}\ m^{-1}$.[33] This can be explained by the very low concentration of the nanoparticles, which was less than 0.3 mass%.

The hardness of the EF-Cu specimen was approximately 70 Hv, which is much higher than the value of 45 Hv obtained for well-annealed pure copper. This is attributable to the hardening induced by the fine grains of the EF-Cu specimen.[29] The hardness values of the EF-Cu/SiO_2, EF-Cu/ZrO_2, and EF-Cu/CeO_2 specimens were not significantly different from that of the EF-Cu specimen owing to their lack of oxide nanoparticles. The hardness was increased slightly to 80 Hv for the EF-Cu/Al_2O_3 specimen, but a far more significant (90%) increase to 135 Hv was observed for the EF-Cu/TiO_2 specimen.

Figure 4 shows representative nominal stress–strain curves for the EF-Cu and EF-Cu/TiO_2 specimens subjected to tensile testing. Table III summarizes the 0.2% yield strength, ultimate tensile strength, elongation to fracture, and Young's modulus for the two specimens. It can be seen that the yield strength (250 MPa) and ultimate tensile strength (302 MPa) of the EF-Cu/TiO_2

https://doi.org/10.1557/jmr.2014.401 Published online by Cambridge University Press

specimen are notably greater than those of the EF-Cu specimen. This means that the mechanical strength could be improved without significant degradation of the electrical conductivity, although the elongation to fracture was decreased by a few percent.

On the basis of the microstructural information presented thus far, the mechanism by which strengthening is attained through a dispersion of TiO_2 nanoparticles can be explained as follows. First, according to the Orowan mechanism, dislocations in the copper matrix must bypass any embedded TiO_2 nanoparticles, as these are much harder than the matrix. The strengthening induced by such nondeformable particles is given by the Ashby–Orowan equation[4,5]

$$\Delta\sigma_p = \left(0.538Gbf^{1/2}/d\right)\ln[d/(2b)] \quad , \qquad (1)$$

where G is the shear modulus of the copper matrix, b is the magnitude of the Burgers vector, f is the volume fraction of the particles, and d is the effective diameter of the circular cross-section of the obstacle particles. Assuming that the nanoparticles are uniformly dispersed in the matrix, d can be regarded as equivalent to the mean size of the TiO_2 nanoparticles, 15 nm (Fig. 1). The volume fraction (f) of TiO_2 particles was calculated to be 0.61% using a density of 4.27 g/cm^2, and the mass fraction listed in Table I. By inserting G = 48.3 GPa and b = 0.255 nm[34] for copper in Eq. (1), $\Delta\sigma_p$ arising from the dispersion of TiO_2 nanoparticles was estimated to be 117 MPa. This provides a qualitative estimate of the contribution of TiO_2 nanoparticles to the strengthening of the copper matrix, but it does quantitatively differ from the measured $\Delta\sigma_p$ (approximately 70 MPa in 0.2% yield stress) that was calculated from Table III. This discrepancy must be the result of the nonuniform dispersion and partial agglomeration of the embedded TiO_2 nanoparticles that are evident in Fig. 2(d), suggesting that the strength of the copper-matrix composites could be further enhanced if this agglomeration of nanoparticles is controlled. In addition, the potential, at least according to Eq. (1), could further increase the concentration of TiO_2 nanoparticles. These modifications of the electroforming process will form the basis of a future paper. It should be noted that the Young's modulus of the EF-Cu/TiO_2 specimen was also greater than that of the EF-Cu specimen (Table III). This is possibly because of the high Young's modulus of anatase TiO_2, which has been reported to be more than 150 GPa,[35] although further work is needed to confirm the hypothesis.

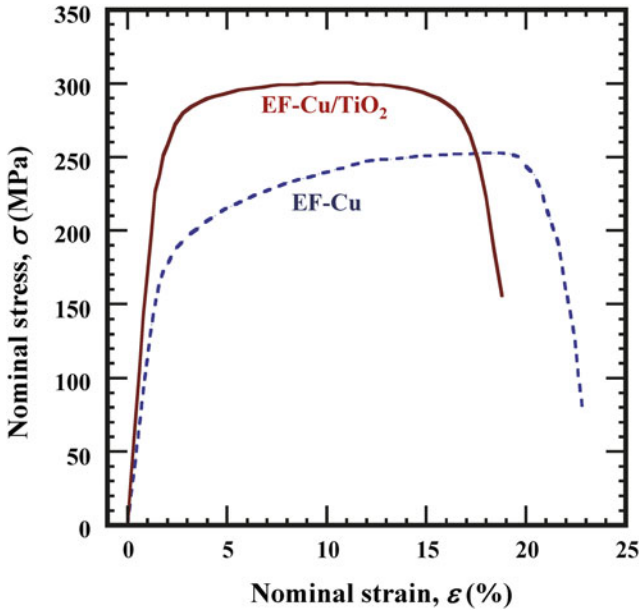


FIG. 4. Typical nominal stress–strain curves for EF-Cu and EF-Cu/TiO_2 composites.

TABLE III. 0.2% yield strength, ultimate tensile strength, elongation to fracture, and Young's modulus of EF-Cu and EF-Cu/TiO_2 composites.

Specimen	0.2% yield strength, σ_y (MPa)	Ultimate tensile strength, σ_{UTS} (MPa)	Elongation to fracture, ε_f%	Young's modulus, E (GPa)
EF-Cu/TiO_2	250 ± 18	302 ± 16	18 ± 2	142 ± 12
EF-Cu	180 ± 13	252 ± 7	21 ± 3	114 ± 3

IV. CONCLUSION

Copper-matrix composites containing dispersed oxide nanoparticles were prepared by electroforming in a copper sulfate–sulfuric acid solution containing 1 cm^3/L of the nanoparticles. From an evaluation of its microstructure and mechanical and electrical properties, the following conclusions were obtained:

(1) Nanoparticle-reinforced copper-matrix composites can be electroformed using an electrolyte containing TiO_2 or possibly Al_2O_3 nanoparticles. However, it is difficult to obtain such a composite using SiO_2, ZrO_2, or CeO_2 nanoparticles in a surfactant-free electrolyte. This can be explained by the nature of the surface potential: TiO_2 has a positive zeta potential in the electrolyte solution, whereas SiO_2, ZrO_2, and CeO_2 have negative zeta potentials. The zeta potential of Al_2O_3 nanoparticle is near neutral.

(2) The electrical conductivity of the EF-Cu/TiO_2 specimen is not significantly different from that of pure copper, as the TiO_2 nanoparticles amount to less than 0.3 mass% (0.6% by volume) of the total composite. Nevertheless, the hardness, yield, and ultimate tensile strength are significantly improved by the TiO_2 nanoparticles primarily owing to strengthening by Orowan mechanics.

https://doi.org/10.1557/jmr.2014.401 Published online by Cambridge University Press

ACKNOWLEDGMENTS

The authors are grateful to Prof. Y. Takigawa and Prof. S. Yagi of Osaka Prefecture University (OPU) and Y. Nakai, Dr. T. Kuwabara, and A. Inoue of Sumitomo Electric Industries Ltd. for their valuable discussions and comments. The authors also wish to thank E. Aoyagi and Y. Hayasaka of the Institute for Materials Research of Tohoku University, and S. Shiraishi of OPU for their technical assistance. Financial support was provided by the Japan Society for the Promotion of Science (JSPS) through a Grant-in-Aid for Scientific Research (C) (No. 26420663).

REFERENCES

1. S. Nagarjuna, K. Balasubramanian, and D.S. Sarma: On the variation of mechanical properties with solute content in Cu–Ti alloys. *Mater. Sci. Eng., A* **225**, 118 (1999).
2. J. Miyake and M.E. Fine: Electrical conductivity versus strength in a precipitation hardened alloy. *Acta Metall. Mater.* **40**, 733 (1992).
3. S. Semboshi and T.J. Konno: Effect of aging in hydrogen atmosphere on electrical conductivity of Cu-3 at.% Ti alloy. *J. Mater. Res.* **23**, 473 (2008).
4. T. Gladman: Precipitation hardening in metals. *Mater. Sci. Technol.* **15**, 30 (1999).
5. Z. Zhang and D.L. Chen: Consideration of Orowan strengthening effect in particulate-reinforced metal matrix nanocomposites: A model for predicting their yield strength. *Scr. Mater.* **54**, 1321 (2006).
6. V. Viswanathan, T. Laha, K. Balani, A. Agarwal, and S. Seal: Challenges and advances in nanocomposite processing techniques. *Mater. Sci. Eng., R* **54**, 121 (2006).
7. H. Xing, X. Cao, W. Hu, L. Zhao, and J. Zhang: Interfacial reactions in 3D-SiC network reinforced Cu-matrix composites prepared by squeeze casting. *Mater. Lett.* **59**, 1563 (2005).
8. C.S. Ramesh, R. Noor Ahmed, M.A. Mujeebu, and M.Z. Abdulah: Development and performance analysis of novel cast copper–SiC–Gr hybrid composites. *Mater. Des.* **30**, 1957 (2009).
9. M. Barmouz, P. Asadi, M.K. Besharati Givi, and M. Taheirishargh: Investigation of mechanical properties of Cu/SiC composite fabricated by FSP: Effect of SiC particles' size and volume fraction. *Mater. Sci. Eng., A* **528**, 1740 (2011).
10. A. Afshar and A. Simchi: Abnormal grain growth in alumina dispersion-strengthened copper produced by an internal oxidation process. *Scr. Mater.* **58**, 966 (2008).
11. A. Fathy, F. Shehata, M. Abdelhameed, and M. Elmahdy: Compressive and wear resistance of nanometric alumina reinforced copper matrix composites. *Mater. Des.* **36**, 100 (2012).
12. K. Mizuuchi, K. Inoue, Y. Agari, Y. Morisada, M. Sigioka, M. Tanaka, T. Takeuchi, M. Kawahara, and Y. Makino: Processing of diamond particle dispersed aluminium matrix composites in continuous solid-liquid co-existent state by SPS and their thermal properties. *Composites, Part B* **42**, 10 (2011).
13. J. Naser, W. Riehemann, and H. Ferkel: Dispersion hardening of metals by nanoscaled ceramic powders. *Mater. Sci. Eng., A* **234**, 467 (1997).
14. S. Mula, P. Sahani, S.K. Pratihar, S. Mal, and C.C. Koch: Mechanical properties and electrical conductivity of Cu–Cr and Cu–Cr–4% SiC nanocomposites for thermo-electric application. *Mater. Sci. Eng., A* **528**, 4348 (2011).
15. E.S. Chen, G.R. Lakshminarayanan, and F.K. Sautter: The codeposition of alumina and titania with copper. *Metal. Trans.* **2**, 937 (1971).
16. C. Buelens, J.P. Celis, and J.R. Roos: Electrochemical aspects of the codeposition of gold and copper with inert particles. *J. Appl. Electrochem.* **13**, 541 (1983).
17. C.C. Lee and C.C. Wan: A study of the composite electrodeposition of copper with alumina powder. *J. Electrochem. Soc.* **135**, 1930 (1988).
18. M. Musiani: Electrodeposition of composites: An expanding subject in electrochemical materials science. *Electrochim. Acta* **45**, 3397 (2000).
19. J. Zhu, L. Liu, G. Hu, B. Shen, W. Hu, and W. Ding: Study on composite electroforming of Cu/SiC_p composites. *Mater. Lett.* **58**, 1634 (2004).
20. M. Verelst, J.P. Bonino, and A. Rousset: Electroforming of metal matrix composite: Dispersoid grain size dependence of thermostructural and mechanical properties. *Mater. Sci. Eng., A* **135**, 51 (1991).
21. J.H. Zhu, H.Z. Liu, L. Liu, H.J. Zhao, B. Shen, and W.B. Hu: Preparation and characterization of electroformed Cu/nano Al_2O_3 composite. *Mater. Sci. Technol.* **23**, 665 (2007).
22. S. Ramalingam, V.S. Muralidharan, and A. Subramania: Electrodeposition and characterization of Cu–TiO_2 nanocomposite coatings. *J. Solid State Electrochem.* **13**, 1777 (2009).
23. V. Mangam, K. Das, and S. Das: Structure and properties of electrocodeposited Cu–CeO_2 nanocomposite thin film. *Mater. Chem. Phys.* **120**, 631 (2010).
24. A. Robin, J.C.P. Santana, and A.F. Sartori: Characterization of copper–silicon nitride composite electrocoatings. *J. Appl. Electrochem.* **40**, 507 (2010).
25. H. Zhao, L. Liu, Y. Wu, and W. Hu: Investigation on wear and corrosion behavior of Cu–graphite composites prepared by electroforming. *Compos. Sci. Technol.* **67**, 1210 (2007).
26. A. Ibanez and E. Fatas: Mechanical and structural properties of electrodeposited copper and their relation with the electrodeposition parameter. *Surf. Coat. Technol.* **191**, 7 (2005).
27. R. Winand: Electrodeposition of metals and alloys—New results and perspectives. *Electrochim. Acta* **39**, 1091 (1994).
28. A. Cziraki, I. Gerocs, E. Toth-Kadar, and I. Bakonyi: TEM and XRD study of the microstructure of nanocrystalline Ni and Cu prepared by severe plastic deformation and electrodeposition. *Nanostruct. Mater.* **6**, 547 (1995).
29. M. Hakamada, Y. Nakamoto, H. Matsumoto, H. Iwasaki, Y. Chen, H. Kusuda, and M. Mabuchi: Relationship between hardness and grain size in electrodeposited copper films. *Mater. Sci. Eng., A* **457**, 120 (2007).
30. T. Mattson, M. Sedin, and H. Theliander: Zeta-potential and local filtration properties: Constitutive relationships for TiO_2 from experimental filtration measurements. *Chem. Eng. Sci.* **66**, 4573 (2011).
31. P. Velikovska and P. Mikulasek: The influence of Cl^-, SO_4^{2-} and PO_4^{3-} ions on the ζ-potential and microfiltration of titanium dioxide dispersions. *Sep. Purif. Technol.* **58**, 295 (2007).
32. H. Simunkova, P. Pessenda-Garcia, J. Wosik, P. Angerer, H. Kronberger, and G.E. Nauer: The fundamentals of nano- and submicro-scaled ceramic particles incorporation into electrodeposited nickel layer: Zeta potential measurements. *Surf. Coat. Technol.* **203**, 1806 (2009).
33. K. Pomoni, M.V. Safianou, T. Georgakopoulos, N. Boukos, and C. Trapalis: Electrical conductivity studies of anatase TiO_2 with dominant highly reactive {001} facets. *J. Alloys Compd.* **548**, 194 (2013).
34. S. Semboshi, T. Nishida, and H. Numakura: Microstructure and mechanical properties of Cu–3 at.% Ti alloy aged in a hydrogen atmosphere. *Mater. Sci. Eng., A* **517**, 105 (2009).
35. I. Borgese, M. Gelfi, E. Bontempi, P. Goudeau, G. Geandier, D. Thiaudiere, and L.E. Depero: Young modulus and Poisson ratio measurements of TiO_2 thin film deposited with atomic layer deposition. *Surf. Coat. Technol.* **206**, 2459 (2012).

https://doi.org/10.1557/jmr.2014.401 Published online by Cambridge University Press